J Incl Phenom Macrocycl Chem (2008) 61:41–51
DOI 10.1007/s10847-007-9391-3

ORIGINAL ARTICLE

Inclusion complexes of Sulconazole with β-cyclodextrin and hydroxypropyl β-cyclodextrin: characterization in aqueous solution and in solid state

Mariana Spulber · Mariana Pinteala · Valeria Harbagiu · Bogdan C. Simionescu

Received: 20 April 2007 / Accepted: 24 November 2007 / Published online: 15 December 2007
© Springer Science+Business Media B.V. 2007

Abstract Complexation between sulconazole (SULC), an imidazole derivative with in vitro antifungal and antiyeast activity, and β-cyclodextrins (β-CD and HP-β-CD) was studied in solution and in solid states. Complexation in solution was evaluated using solubility studies and nuclear magnetic resonance spectroscopy (^{1}H-NMR). In the solid state, differential scanning calorimetry (DSC), thermal gravimetric analysis (TGA), scanning electron microscopy (SEM) and RX diffraction studies were used. Solubility studies suggested the existence of inclusion complex between SULC and β-CD or HP-β-CD. ^{1}H-NMR spectroscopy studies showed that the complex formed occurs by complexation of imidazole ring into inner cavity. DSC studies showed the existence of a complex of SULC with β-CD. The TGA and RX studies confirmed the DSC results of the complex. Solubility of SULC in solid complexes was studied by the dissolution method and it was found to be much more soluble than the uncomplexed drug.

Keywords Cyclodextrin · Sulconazole · Inclusion complex

Introduction

Cyclodextrins (CDs) and modified cyclodextrins act as host molecules to form inclusion complexes rather non-specifically with a wide variety of guest molecules. Complexation of guest compounds with CDs or modified cyclodextrins can alter guest solubility, increase stability against the effects of light, heat, and oxidation, mask unwanted physiological effects, and reduce volatility [1]. The most common application of CDs in the pharmaceutical industry is to enhance drug solubility, dissolution rate, and bioavailability of poorly water-soluble drugs. A large variety of drugs encapsulated through noncovalent interactions into unmodified or modified CDs (especially hydroxypropyl-β-cyclodextrin (HP-β-CD)) cavity were described [2].

Sulconazole nitrate is an imidazole derivative with in vitro antifungal and antiyeast activity called (+)-1-[2,4-dichloro-*b*-[(*p*-chlorobenzyl)-thio]-phenethyl] imidazole mononitrate. Sulconazole nitrate is a broad-spectrum antifungal agent intended for topical application.

Sulconazole nitrate is a white to off-white crystalline powder with a molecular weight of 460.77. It is freely soluble in pyridine, slightly soluble in ethanol, acetone, and chloroform: and very slightly soluble in water (1.9 mg/mL). It has a melting point of about 130 °C.

Sulconazole is used to treat skin infections such as athlete's foot, jock itch, and ringworm. Like all azole antifungals, it inhibits the fungal cytochrome P-450 3-A dependent enzyme 14-alpha demethylase, thereby interrupting the synthesis of ergosterol. Inhibition of this critical enzyme in the ergosterol synthesis pathway leads to the depletion of ergosterol in the cell membrane and accumulation of toxic intermediate sterols, causing increased membrane permeability and inhibition of fungal growth [3]. Azole antifungals can also inhibit many mammalian cytochrome P450-dependent enzymes involved in hormone synthesis or drug metabolism [4]. Therefore, azole antifungals are particularly susceptible to clinically significant

M. Spulber (✉) · M. Pinteala · V. Harbagiu · B. C. Simionescu
Inorganic Polymers, Institute of Macromolecular Chemistry
Petru Poni, Str. Gr Ghica Voda, no 41 A, Iasi 711321, Romania
e-mail: mari_19ian@yahoo.com

drug interactions with other medications metabolized through the P450 pathway [5].

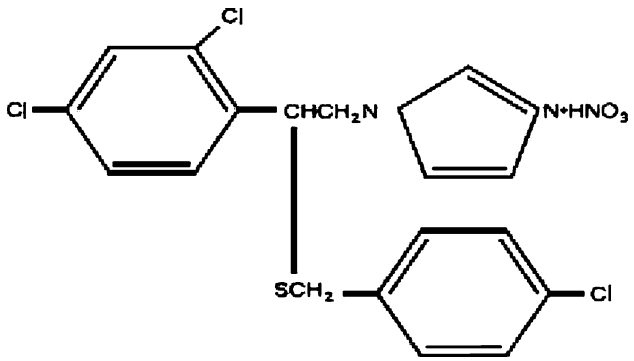

Sulconazole nitrate has a broad-spectrum antifungal activity that inhibits the in vitro growth of the common pathogenic dermatophytes including *Trichophyton rubrum*, *Trichophyton mentagrophytes*, *Epidermophyton floccosum*, and *Microsporum canis*. It also inhibits (in vitro) the organism responsible for *Tinea versicolor*, *Malassezia furfur*. Sulconazole nitrate has also been shown to be active in vitro against *Candida albicans* and certain gram positive bacteria.

A modified Draize test showed no allergic contact dermatitis and a phototoxicity study showed no phototoxic or photoallergic reaction to sulconazole nitrate cream. Maximization tests with sulconazole nitrate cream showed no evidence of contact sensitization or irritation [3]. There were no systemic effects and only some cutaneous adverse sulconazole may cause side effects including: itching, rash, burning, irritation or stinging, redness.

There are no adequate and well-controlled studies in pregnant women. Sulconazole nitrate should be used during pregnancy only if clearly needed. Sulconazole nitrate has been shown to be embryotoxic, it was not teratogenic in rats or rabbits. Sulconazole nitrate given orally to rats resulted in prolonged gestation and dystocia. Several females died during the prenatal period, most likely due to labor complications [6].

Complexation of sulconazole with cyclodextrin offers the possibility to improve the aqueous solubility of sulconazole without modification of its original structure. This may allow a homogeneous delivery system of sulconazole increasing its bioavailability. We synthesized β-cyclodextrin-sulconazole nitrate (β-CD-SULC) and hydroxypropyl-β-cyclodextrin- sulconazole nitrate (HP-β-CD-SULC) inclusion complexes, in order to make it more available for the yeast metabolism, and to reduce consequently the dosage, the treatment period and the gravity of all possible side effects.

Materials and methods

Materials

Sulconazole nitrate (SULC) (Fluka) it was used as given. β-CD and HP-β-CD were obtained from Cyclolab. Double distilled water was used throughout the study.

Methods

Solubility studies

Solubility studies were carried out according to the Higuchi and Connors method [7]. β-CD or HP-β-CD solutions of different concentrations ($0.33–24.6 \times 10^{-4}$ M) were added to a supersaturated solution of SULC and shaken at room temperature (22 ± 1 °C) for 24 h. After reaching equilibrium, the solutions were filtered. The absorbance of solutions containing different mole fraction of the drug and β-CD or HP-β-CD was measured by UV at 190 nm and the concentration of SULC in the each solution was determined with reference to a suitably constructed standard curve.

The apparent stability constant was calculated from initial straight portion of the phase solubility diagram using the Eq. 1 [7].

$$K1{:}1 = \text{slope}/So\ (1 - \text{slope}) \quad (1)$$

where So is the solubility of SULC in the absence of β-CD or HP-β-CD, *slope* is the slope of the experimental phase solubility diagram for β-CD-SULC or HP-β-CD-SULC.

Preparation of the solid complex

The inclusion complexes (C_s) were prepared by freeze drying method. An aqueous solution containing SULC and β-CD or SULC and HP-β-CD in a 1:1 molar ratio was frozen by immersion in liquid nitrogen and freeze-dried in a Martin Christ, ALPHA 1-2LD Freeze-Dryer. The aqueous solutions were obtained by dissolving 4.34×10^{-4} mol SULC and 4.34×10^{-4} mol cyclodextrin in 25 mL distilled water and stirring it at room temperature for 48 h.

Preparation of the physical mixture

(Ph.M) was performed by mixing the powders in a 1:1 molar ratio in a ceramic mortar.

Complex characterization

UV measurements were performed on a Analytik Jena Specord 200 Spectrophotometer.

Differential scanning calorimetry (DSC)

DSC data were obtained using a Perkin Elmer-Diamond device. Each sample (2–6 mg) was exactly weighted in an aluminum pan and was heated at a rate of 10 °C/min between 30 and 330 °C, under nitrogen gas flow. Also, from DSC data it was calculated the inclusion ratio of sulconazole into CD cavity using Eq. 2.

$$\text{Inclusion ratio} = \Delta H_1 \times 100/\Delta H_2 \quad (2)$$

where

- ΔH_1 represents drug discomposure enthalpy in the inclusion complex,
- ΔH_2 represents free drug discomposure enthalpy,
- ΔH_1 and ΔH_2 were obtained for the same amount of pure drug and complexed drug (2.5 mg).

Thermal gravimetric analysis (TGA)

Thermal analyses were performed on freeze-dried samples obtained directly from the preparation medium and TGA data were obtained using a Q-1500 D MomBudapest derivatograph, with System F Paulik, L Eredey.

Nuclear magnetic resonance (^{1}H-NMR)

Nuclear magnetic resonance studies were performed in dimethylsulfoxide on a Bruker Advance DRX 400 device The NOE measurements were performed using a NOE-DIFF-QNP-34 program at room temperature, without degassing. The ROESY spectrum was performed on a Bruker 300 MHz by courtesy of Prof. Philippe Guegan.

Scanning electron microscopy (SEM)

SEM micrographs were obtained on a Tesla Scanning Electron Microscope.

X-ray diffraction (XRD)

XRD patterns were obtained on a Bruker AXS D8 advance RX diffractometer.

Results and discussion

Phase solubility studies

The solubility of SULC in water is very low, 1.9 mg mL^{-1} at 25 °C, as described in literature [6]. In Fig. 1 it is shown the solubility curve obtained for SULC in presence of β-CD (Fig. 1a) and HP-β-CD (Fig. 1b) in distilled water. As it can be seen, SULC solubility in water presents a linear growth, the resulting linear curve can be classified, in general, as an AL type (linear positive isotherm), as described in literature [7]. Since the slope of the two diagrams are less than 1 (0.1562 for SULC-β-CD and 0.1413 for SULC-HP-β-CD) was assumed that the stoichiometry of each complex is 1:1 according to Higuchi and Connors [7]. The apparent solubility constant, K1:1, of each complex was calculated from the correspondent curve of Fig. 1. according to Eq. 1 and it was found to be 74.30 for SULC-β-CD and 30.45 for SULC-HP-β-CD.

A significant increase in dissolution rate can be observed by analyzing Higuchi phase solubility diagrams, which can be explained due to the formation of the complex.

Differential scanning calorimetry

DSC reveals some information on solid-state interactions between drug and cyclodextrins. The DSC thermograms of pure components and of the β-CD-SULC inclusion complex are presented in Fig. 2. A typical DSC curve for a crystalline anhydrous substance, with a sharp fusion endotherm (T peak = 135 °C), was obtained for SULC. Liberation of crystal water from β-CD is observed as a broad endothermal peak, around 100 °C. The characteristic

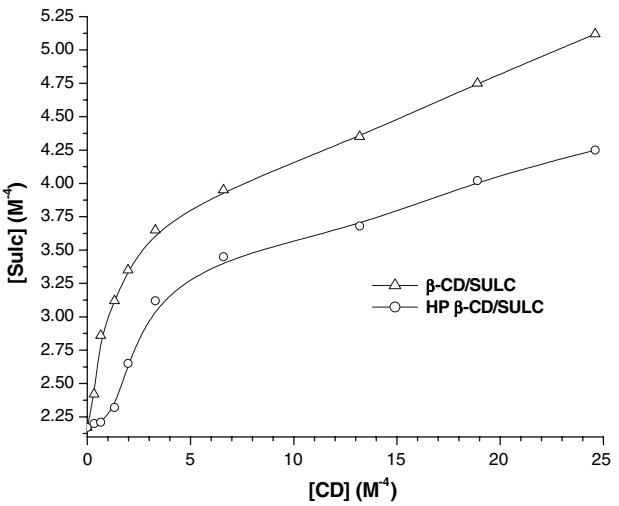

Fig. 1 Higuchi phase solubility diagram of SULC in presence of β-CD and in presence of HP-β-CD

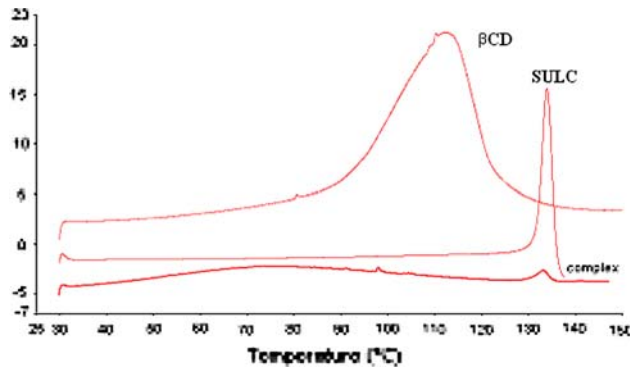

Fig. 2 DSC thermograms of β-CD, SULC, and β-CD-SULC (complex)

thermal peak of the drug appears at 136.5 °C, but it is strongly reduced in intensity and somewhat broadened in complex, modification that can be attributed to an inclusion complexation process.

Analyzing decomposition enthalpies obtained for the pure and included drug we calculated inclusion ratio with Eq. 2. We estimated that the inclusion ratio for the complexes β-CD-SULC varies around 76.02%.

The DSC thermograms of pure drug and of HP-β-CD-SULC inclusion complexes are presented in Fig. 3. The DSC curve of sulconazol is typical of a crystalline anhydrous substance, with a sharp fusion endotherm (T peak = 135 °C). Liberation of crystal water from HP-β-CD is observed as a broad endothermal peak, at around 90 °C. HP-β-CD is an amorphous material, and does not exhibit a melting point, as would be observed for crystalline materials. The characteristic thermal peak of the drug appeared around 137 °C, but it is strongly reduced in intensity and somewhat broadened in the HP-β-CD-SULC inclusion complexes due to the inclusion complexation process.

Analyzing decomposition enthalpies obtained for the pure and included drug, the calculated inclusion ratio applying Eq.2 was found to be 81.43%.

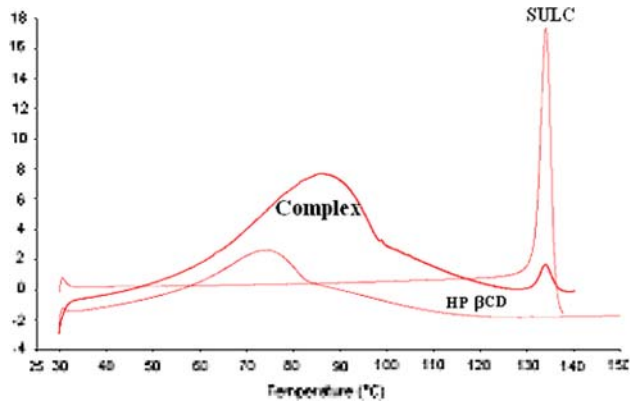

Fig. 3 DSC thermograms of HP-β-CD, SULC, and HP-β-CD-SULC (complex) **(complex)**

Thermal gravimetric analysis

TGA curves are presented in Figs. 4 and 5 and they are describing weight loss of the pure components and of the inclusion complexes obtained by freeze-drying method.

β-CD has the characteristic behavior described in literature, with a loss weight varying from 225 to 250 °C, and the a value of decomposing temperature of 300 °C. Weight loss raises until 150 °C, due to intermolecular water, remains unchanged until 250 °C, and raises again reaching 92.5% at 275 °C.

SULC starts to decompose at 150 °C, weight loss increasing rapidly reaching 48.5% at 300 °C.

The weight loss for the inclusion complex rises from 75 °C until 150 °C is around 7%, and from 250 to 300° C, reaching almost 50.1%, due to increasing of the drug thermal stability.

HP-β-CD has initial decomposition values varying from 250 to 275 °C, with a massive decomposition at 350° C. Weight loss increases at 175 °C (due to water loss), remaining unchanged until 250 ° C, at raises again until 350 °C reaching 75.2%.

Weight loss for the inclusion complex obtained by freeze drying raises from 75 to 150 °C, and from 200 to 300 °C, reaching 63.5% at 300 °C, due to included drug thermal stability increasing from 200 to 300 °C. Cyclodextrin melting point rises from 300 to 325 °C in the inclusion complex, due to complexation process.

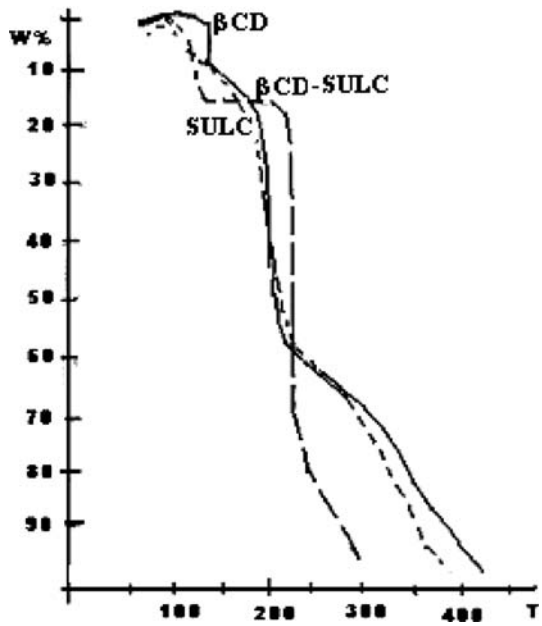

Fig. 4 ATG curves of: β-CD; SULC; βCD-SULC

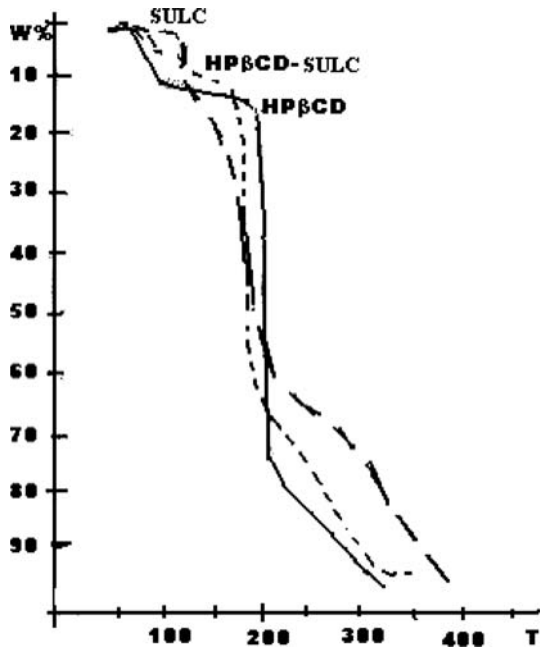

Fig. 5 ATG curves of: HP-β-CD; SULC; HP-β-CD-SULC

Powder X-ray diffraction

X-ray powder, diffraction patterns of pure SULC and β-CD, and corresponding solid inclusion complexes with CD, are shown in Fig. 6. In the X-ray diffractograms of SULC and β-CD powder, sharp diffraction peaks are present, indicating their crystalline state. By contrast the X-ray diffraction patterns of β-CD-SULC system were characterized only by large diffraction peaks, in which it is no longer possible to distinguish the characteristic crystallinity peaks of pure drug or β-CD. These results indicate

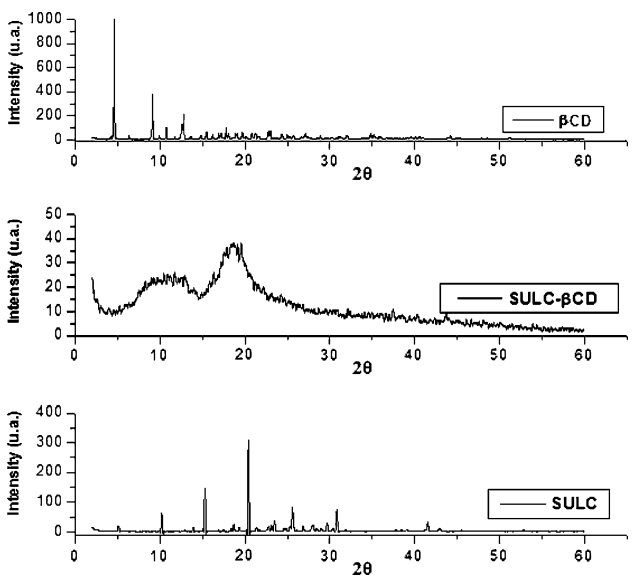

Fig. 6 X-Ray diffraction patterns of: SULC, β-CD, and SULC-β-CD

Table 1 Interplanar distances calculated from X-ray pattern

Sample code	d (Å)
βCD	19.19, 13.88, 8.90, 8.20, 6.90, 5.77, 5.48, 5.43, 4.97, 4.64, 4.50, 4.14, 3.85, 3.57, 3.44, 3.27, 3.07, 2.25
SULC	8.56, 4.34, 2.91, 2.40, 2.20, 2.11, 1.77, 1.70, 1.63, 1.55, 1.50, 1.16
βCD-SULC	8.56, 5.74, 4.70, 4.32, 3.45, 2.87
HP-β-CD	7.77, 4.94, 4.74, 4.52, 2.06
HP-β-CD-SULC	16.68, 7.29, 4.64, 4.32, 3.47, 2.43

that SULC is no longer present as a crystalline material, and its CD solid complexes exist in the amorphous state.

The interplanar distances for the investigated samples are presented in Table 1. The data related to β-CD (see Fig. 6 and Table 1), being compared with the data published in Refs. [8, 9], prove the same structure of β-CD as previously reported. The data related to SULC can be seen from Fig. 6 and Table 1 show also a crystalline structure. As can be seen from Fig. 6 and Table 1, CD-SULC complex has different (individual) structure, showing almost complete β amorphization of the drug and CD. We could recognize only one diffusion reflex ($d = 8.56$ Å from SULC). The formation of an amorphous state proves that the drug was dispersed in a molecular state with CD [10].

The same behavior can be observed analyzing SULC-HP β-CD inclusion complexes. The X-ray diffraction pattern of the inclusion compound differed considerably from that of the drug or of the HP-β-CD alone (Fig. 7). The diffractogram of the complex showed peaks of diminished

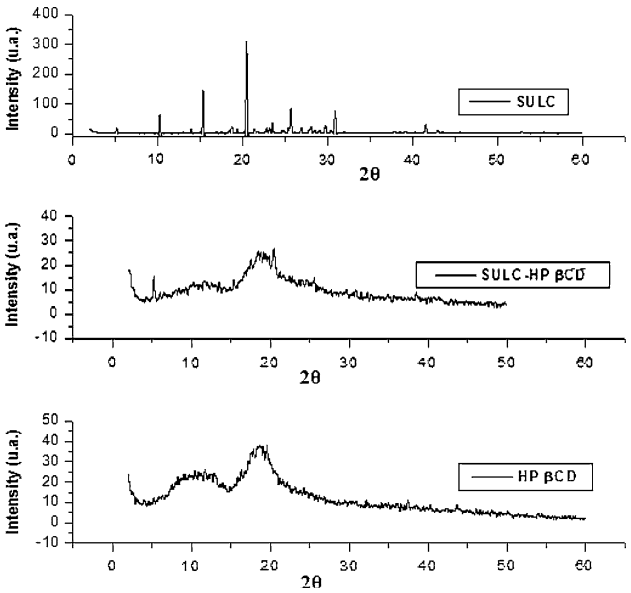

Fig. 7 X-ray diffraction patterns of: SULC, HP-β-CD, and SULC-HP-β-CD

intensity suggesting almost complete amorphisation of the drug (Fig. 7, Table 1). The diffractogram of inclusion complex shows a different crystalline state which is similar to that of the case described anterior.

Scanning electron microscopy (SEM)

This method is not very conclusive method to confirm the formation of complex but it can give us useful informations about the efficiency of the inclusion process it helps to assess the existence of a single component in the complex.

The particle morphology of SULC, β-CD, its physical mixtures, and solid complexes, can be seen in SEM photographs presented in Fig. 8. SULC appeared as cylindrical crystals, tending to form aggregates. β-CD consisted of cylindrical and irregularly shaped crystals. The physical mixtures showed particles of β-CD embedded with SULC particles, and a comparable morphology with pure compounds, taken separately. In contrast, a drastic change in the morphology and change in crystalline nature was observed in 1:1 freeze-dried, products of β-CD with SULC, revealing an apparent interaction in the solid state.

The morphology of SULC, HP-β-CD, and its physical mixtures, and solid complexes, can be seen in SEM photographs presented in Fig. 9. SULC appeared as crystalline crystals, tending to form aggregates. HP-β-CD consisted of shrunken, cylindrical particles. The physical mixtures showed particles of HP-β-CD and SULC, with the same morphology as the pure compounds. The complex presented a different morphology with plate-like crystals, revealing an apparent interaction in the solid state.

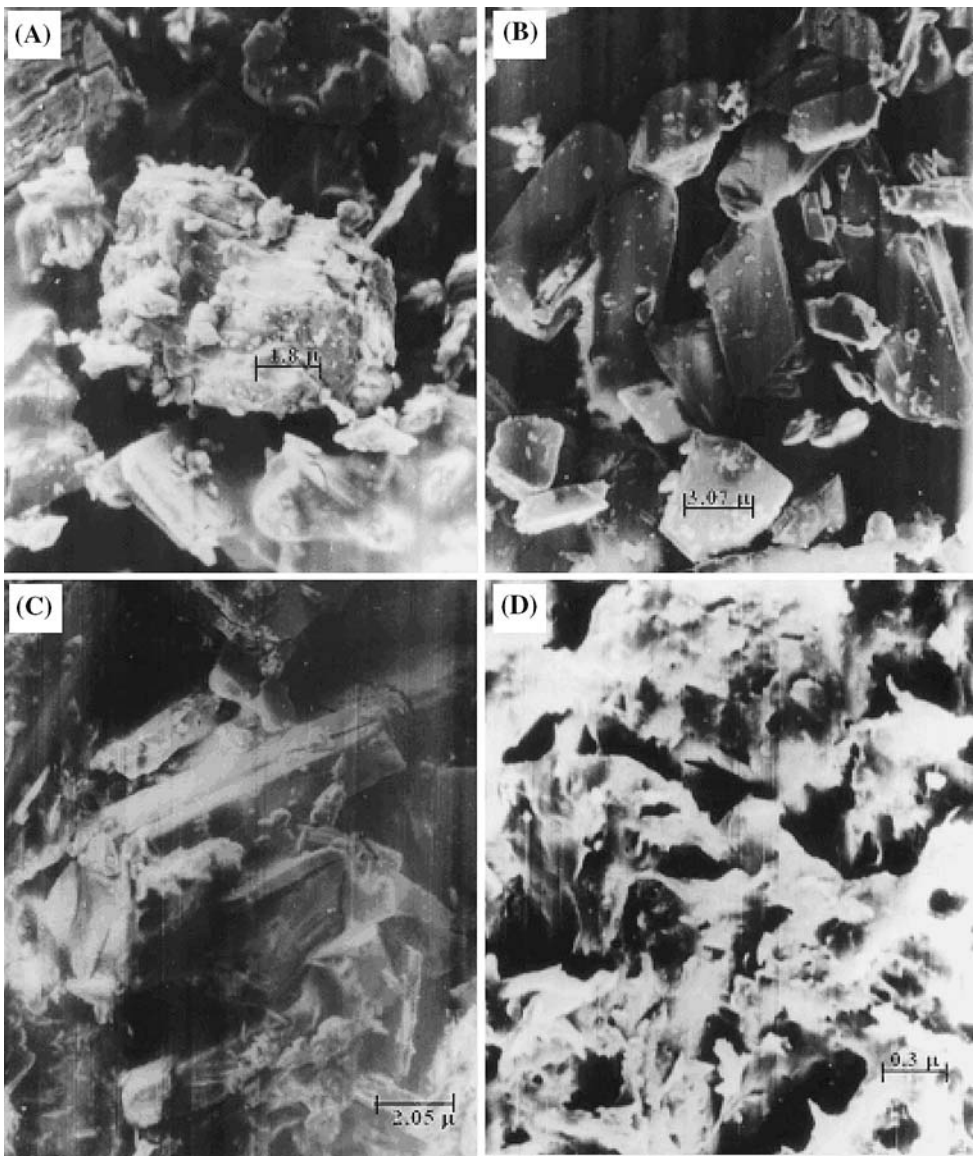

Fig. 8 SEM images of: β-CD (**a**); SULC (**b**); physical mixture of β-CD and SULC (**c**); SULC-β-CD (**d**)

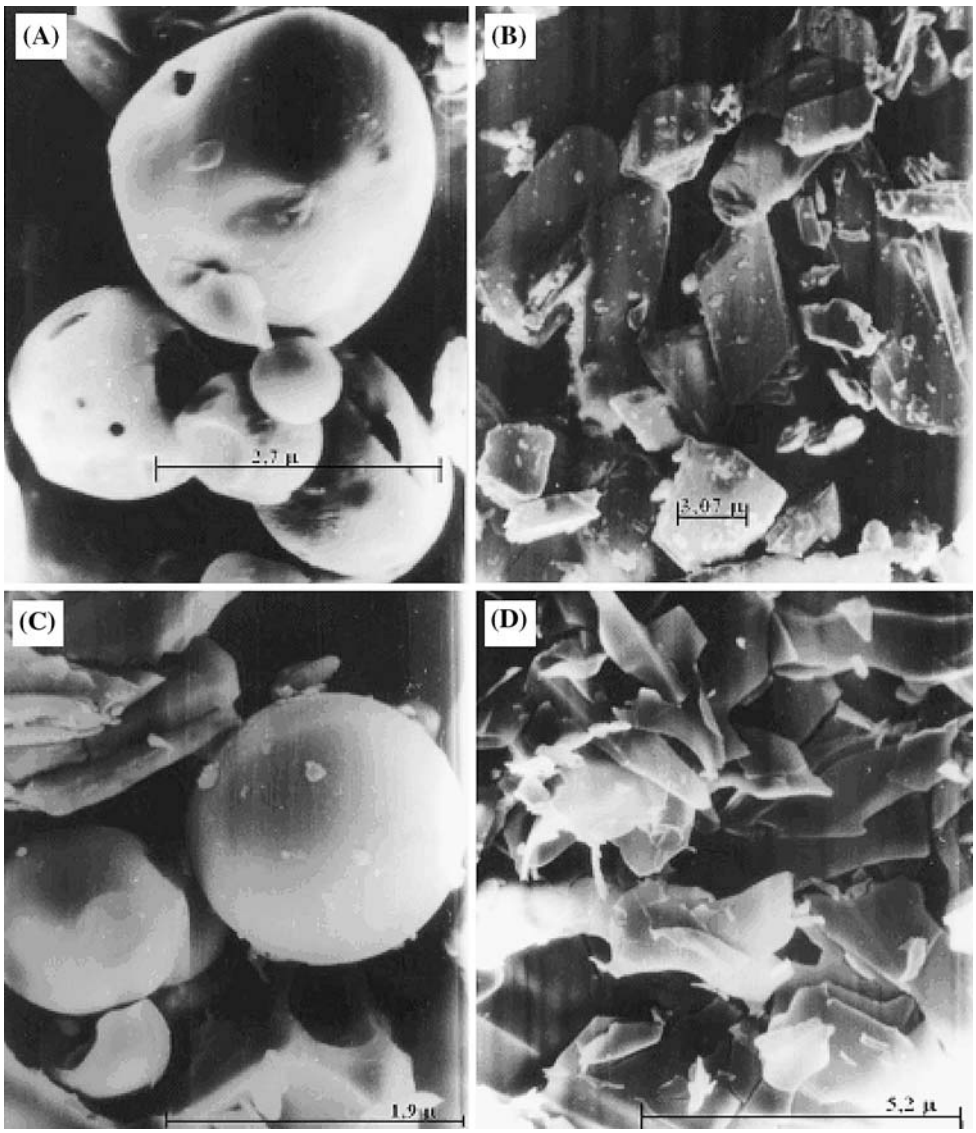

Fig. 9 SEM images of: HP-β-CD (**a**); SULC (**b**); physical mixture of HP-β-CD and SULC (**c**); SULC-HP-β-CD (**d**)

Although solubility studies, Differential Scanning Calorimetry (DSC), Thermal Gravimetric Analysis (TGA), X-ray diffractometry and Scanning Electron Microscopy indicated the existence of complexation between SULC and β-CD and HP-β-CD by freeze-drying method. A deeper insight into the complexation mechanism was obtained from ^{1}H-NMR.

^{1}H-NMR spectroscopy

^{1}H-NMR studies reveal useful information on the nature of the interactions between drug and cyclodextrin in inclusion complexes.

Analyzing the chemical structure of SULC we can suppose the formation of tree type of inclusion complexes, depending on part of SULC (Fig. 10): the dichlorobenzene group (DCB) directly linked to the asymmetric carbon, chlorobenzene-CH_2-S-group (MCB) and protonated imidazole group (IMZ) which could be included alternatively in CD cavity with a more or less pronounced probability. The complexes are respectively notated DCB-β-CD, MCB-β-CD, and IMZ-β-CD.

The ^{1}H-NMR spectra for SULC in the presence of β-CD are compared with the spectra for the individual components and in these cases there are clear differences between the spectra with and without β-CD (Figs. 10, 11, Table 2).

A remarkable upfield shift of Hs8, Hs6, Hs1 of pure SULC in complex shows that the sulconazole penetrate the β-cyclodextrin cavity with a more pronounced probability to form IMZ-β-CD complex and DCB-β-CD when the imidazolic ring penetrates the cavity of CD. The order of the upfield is found to be for SULC: Hs8 (dδ (ppm) = -0.135) > Hs6 (-0.093) > Hs1 (-0.075) > Hs3(-0.051) >

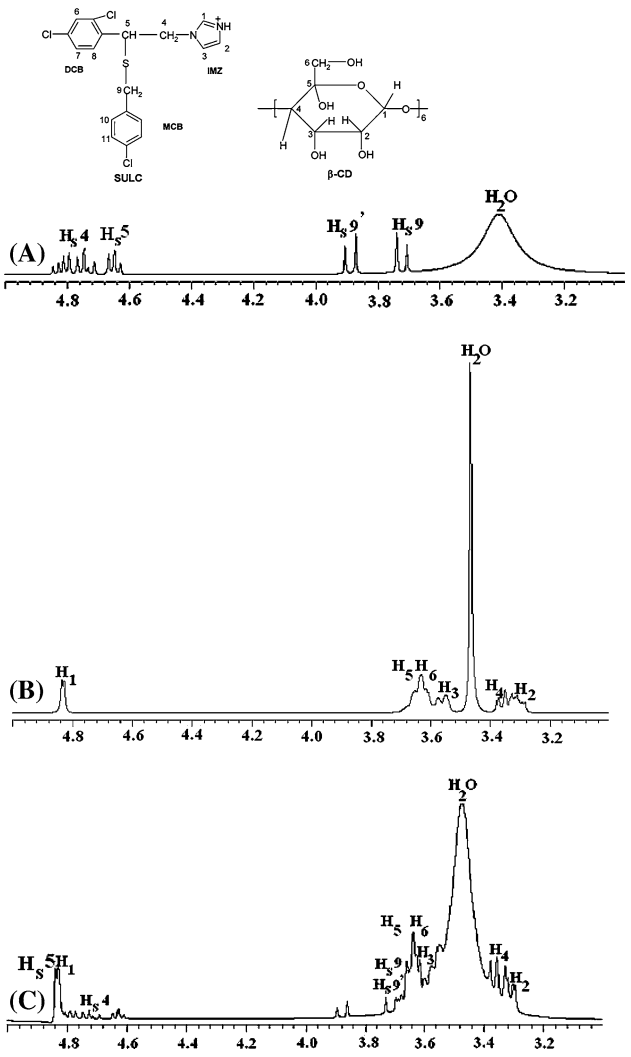

Fig. 10 ^{1}H-NMR spectra in 3.0–5.0 ppm region for SULC (**a**), β-CD (**b**) and β-CD-SULC (**c**)

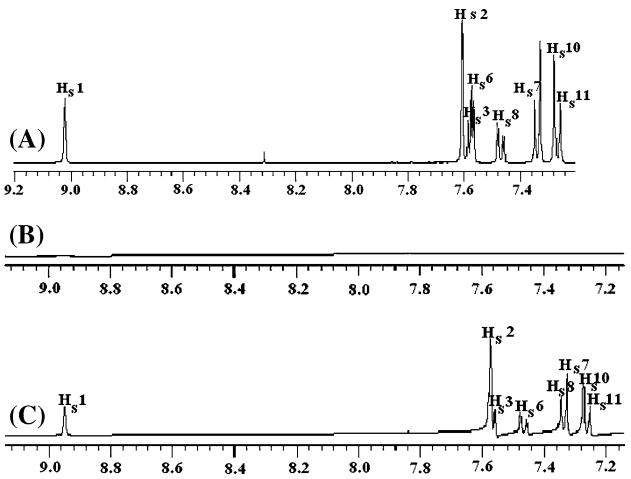

Fig. 11 ^{1}H-NMR spectra in 7.2–9.0 ppm region for SULC (**a**), β-CD (**b**), and β-CD-SULC (**c**)

Table 2 Chemical shift data (δ in ppm) of H-C protons in SULC and β-CD in free state and in the complex state

Code	δ_{free}	$\delta_{complex}$	$d\delta^*$ (ppm)	Observations
SULC				
Hs1	9.021	8.946	−0.075	
Hs2	7.604	7.571	−0.033	
Hs3	7.609	7.558	−0.051	
Hs4	4.740	4.726	−0.014	
Hs5	4.648	4.529	−0.019	
Hs6	7.57	7.477	−0.093	
Hs7	7.347	7.325	−0.022	
Hs8	7.482	7.347	−0.135	
Hs9	3.7215	3.659	−0.062	
Hs10	7.277	7.271	−0.006	
Hs11	7.256	7.251	−0.005	
β-CD				
H_1	4.835–4.826/ 4.8305	4.839–4.830/ 4.8345	+0.004	
H_2	3.317–3.290/ 3.3035	3.329–3.296/ 3.3125	+0.012–0.011/ 0.009	
H_3	3.652–3.608	3.660–3.615	+0.008–0.007	
H_4	3.374–3.351	3.379–3.356	+0.005	
H_5	3.574–3.549/ 3.5615	3.600–3.553/ 3.576	+0.026–0.004/ 0.015	
H_6	3.652–3.608	3.660–3.615	+0.008–0.007	

$d\delta^* = \delta_{complex} - \delta_{free}$

Hs3 (−0.031) > Hs5 (−0.019) > Hs4 (−0.014) > Hs9 (−0.0062) > and Hs10, Hs11 (∼0.005). This remark was made by Piel [10] studying the inclusion of protonated miconazole form in β-CD cavity.

On the other hand a downfield shift of H5 (located inside the cavity [10]) of pure β-CD in complex, as well as a minor modification of H1, H2, H4 can be observed. H3 and H6 of pure CD are overlapped that is why we cannot interpret their shift modifications.

In order to investigate molecular complexes NOE represents a useful tool for a better description of the supramolecular assemblies in solution. NMR NOE studies were developed in order to investigate the inclusion complexes between CD and different drugs [11, 12]. Figure 12 shows the ^{1}H-NMR spectra of β-CD-Sulc complex in comparison with a NOE spectrum obtained after presaturation of H_s1 Sulc protons. A significant nuclear Overhauser enhancement was observed between H_s1, H_s2, H_s3 and H_s4 protons of sulconazole and H_1 and H_5 protons of β-CD suggesting that the inclusion complex was formed probably by the entrance of the IMZ ring of SULC in β-CD cavity.

The ^{1}H-NMR spectra for SULC in the presence of HP-β-CD are compared with the spectra for the individual

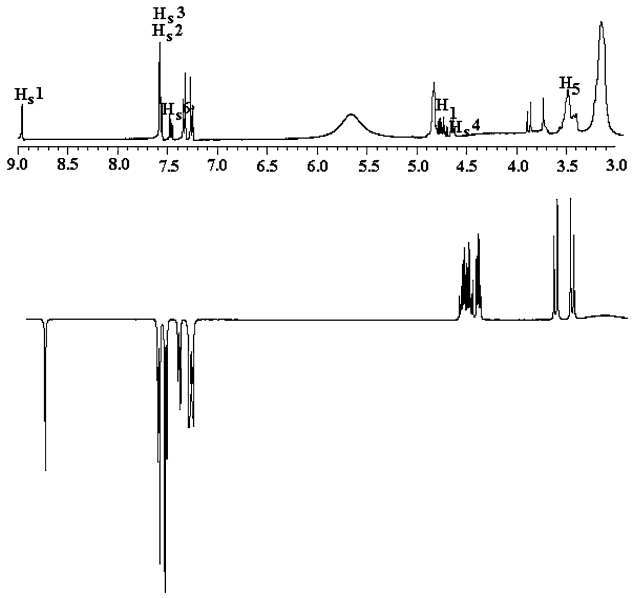

Fig. 12 [1]H-NMR spectra of β-CD-Sulc complex in DMSO and NOE experiment, NOE when H_s1 protons of SULC have been presaturated

components and in these cases there are clear differences between the spectra with and without HP-β-CD (Figs. 13–15 and Table 3).

From Table 3 we can conclude that H3 and H5 protons of HP-β-CD are shifted enough to show the inclusion of the guest inside cavity of cyclodextrin. Also, a remarkable shift of H_s4 and H_s1 of pure SULC in complex show that the SULC penetrates the HP-β-CD cavity with a more pronounced probability to form IMZ/HP-β-CD complex. Considering the data presented in Table 3 the formation of different inclusion complexes is also possible. In addition, a ROESY spectrum in D_2O (Fig. 16) for the sulconazole/HP-β-CD inclusion complexes shows an evident correlation between internal protons of HP-β-CD (H3 and H5, 3.3–3.7 ppm) and the protons of H_s1, H_s2, H_s3 of sulconazole. Similar results have been reported by the other authors [13, 10].

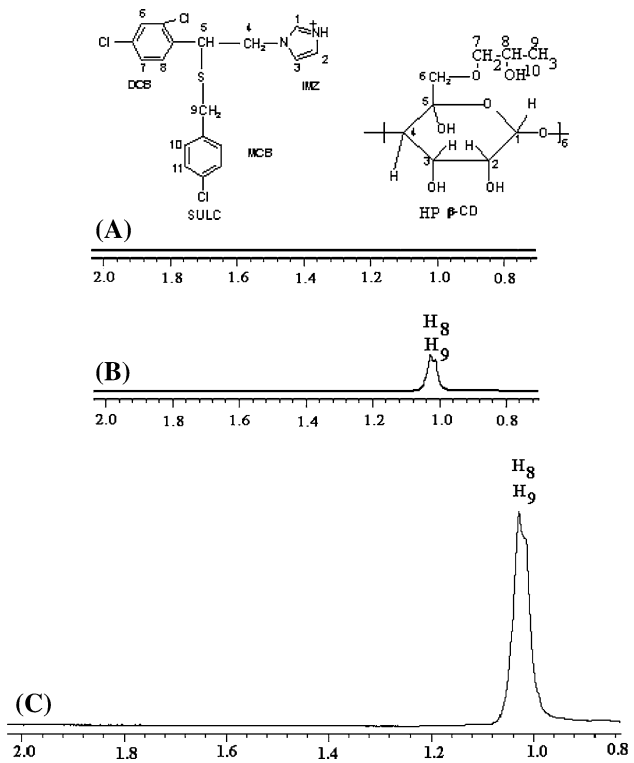

Fig. 13 [1]H-NMR spectra in 0.8–2.0 ppm region for SULC (**a**); HP-β-CD (**b**); HP-β-CD-SULC (**c**)

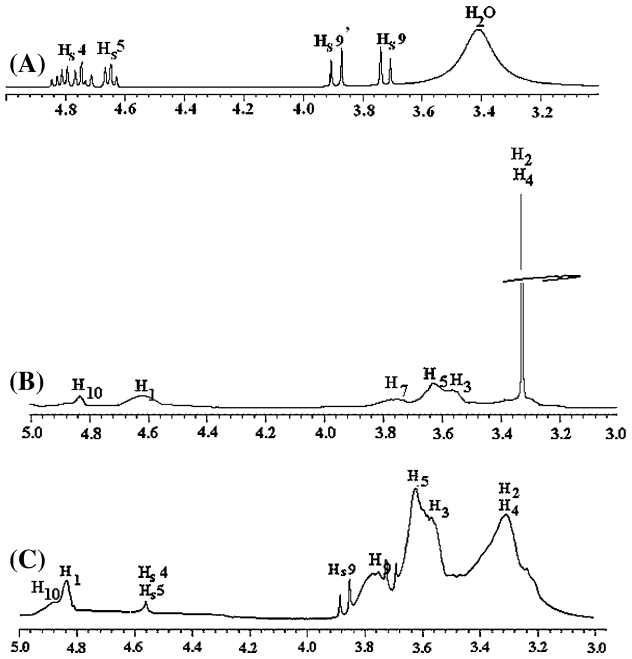

Fig. 14 [1]H-NMR spectra in 3.0–5.0 ppm region for SULC (**a**); HP-β-CD (**b**); HP-β-CD-SULC (**c**)

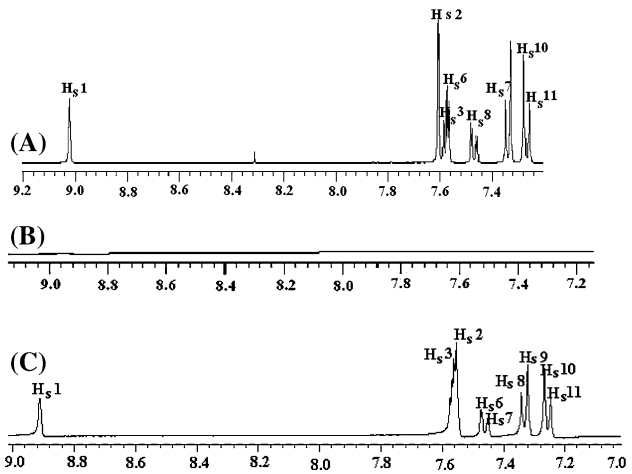

Fig. 15 [1]H-NMR spectra in 7.0–9.0 ppm region for SULC (**a**); HP-β-CD (**b**); HP-β-CD-SULC (**c**)

Table 3 Chemical shift data (δ in ppm) of H-C protons in SULC and HP-β-CD in free state and in the complex state

Code	δ_{free}	δcomplex	dδ^* (ppm)	Observations
SULC				
Hs1	9.021	8.911	−0.110	
Hs2	7.604	7.553	−0.051	
Hs3	7.609	7.561	−0.048	
Hs4	4.740	4.592	−0.148	
Hs5	4.648	4.592	−0.019	
Hs6	7.57	7.468	−0.056	
Hs7	7.347	7.446	−0.022	
Hs8	7.482	7.341	+0.099	
Hs9	3.7215	3.852	+0.132	
Hs10	7.277	7.32	+0.043	
Hs11	7.256	7.265	+0.009	
HP -β-CD				
H_1	4.736–4.766	4.685–4.739	−0.051–0.027	
H_2	3.37–3.563	3.411–3.459	+0.041–0.104	
H_3	3.386	3.569	+0.183	
H_4	3.58	3.509	−0.071	
H_5	3.629	3.725	+0.096	
H_6	3.796	3.798	+0.002	
H_7	1.012–1.027	1.029	0.007–0.002	
H_8	1.012–1.027	1.029	0.007–0.002	
H_9	1.012–1.027	1.029	0.007–0.002	
H_{10}	4.835	4.837	0.002	

$d\delta^* = \delta_{complex} - \delta_{free}$

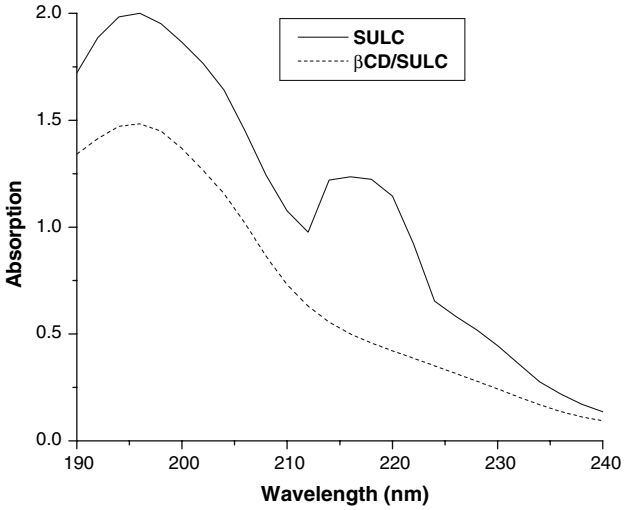

Fig. 17 UV absorption spectra for SULC and its inclusion complex with $\beta\beta$CD in distilled water

UV absorption spectra

UV absorption spectra for the pure drug and the inclusion complexes have been analyzed in distilled water. As it can be seen from Figs. 17, 18 inclusion complexes UV spectra shows the disappearance of the absorption band at 214–218 nm and the movement of the absorption band at 196 nm.

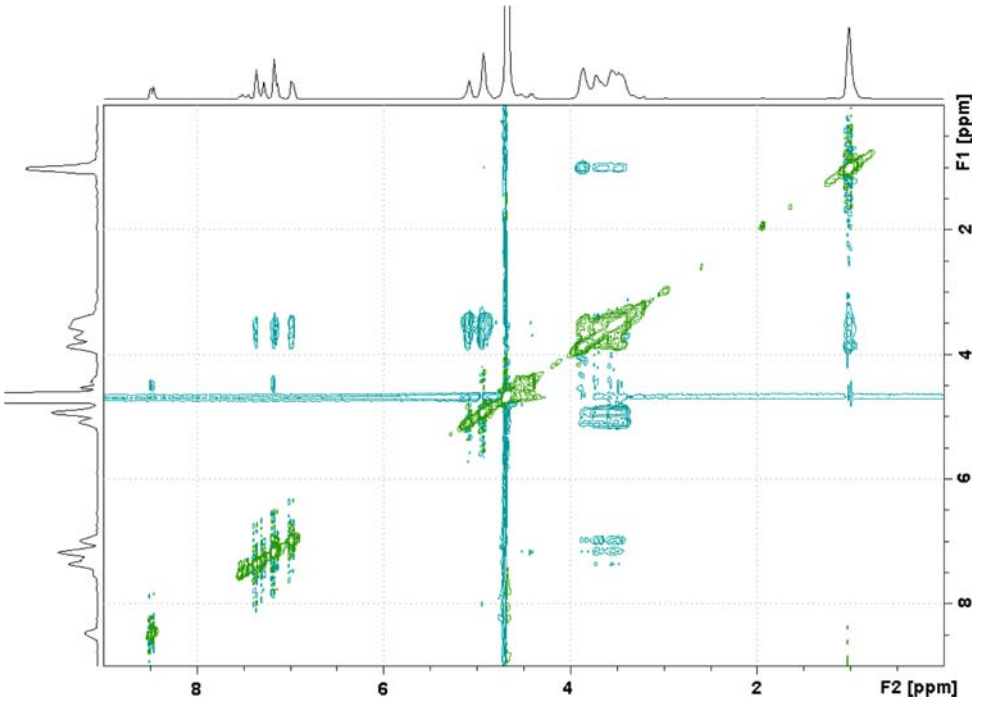

Fig. 16 ROESY spectrum in D_2O for HP-β-CD-SULC inclusion complex

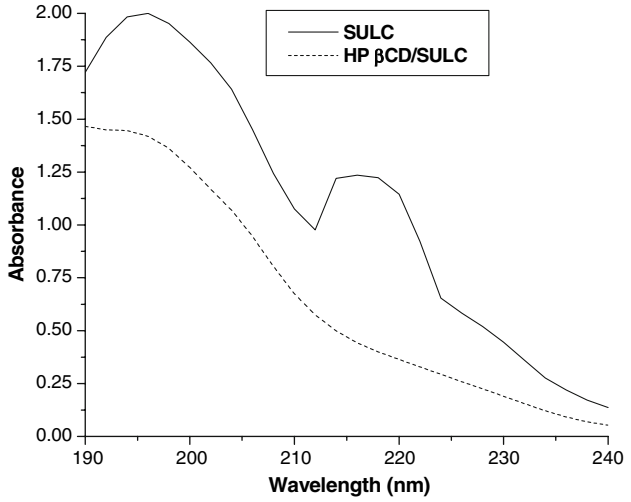

Fig. 18 UV absorption spectra for SULC and inclusion complex SULC-HP βCD in distilled water

Conclusion

Inclusion complexes of sulconazole and β-CD and HP-β-CD were prepared by freeze-drying method in a molar ratio 1:1. This was confirmed by DSC, TGA, NMR, SEM microscopy, UV spectroscopy. Complexation by inclusion increases sulconazole solubility and dissolution. Dissolution increasing is due to the low crystallinity of the complex.

References

1. Hedges, A.R.: Industrial applications of cyclodextrins. Chem. Rev. **98**, 2035–2044 (1998)
2. Loftsson, T., Brewster, M.E.: Pharmaceutical applications of cyclodextrins. 1. Drug solubilization and stabilization. J. Pharm. Sci. **85**, 1017–1025 (1996)
3. Vanden Bossche, H., Marichal, P., Gorrens, J., Bellens, D., Moereels, H., Janssen, P.A.J.: Mutations in cytochrome P450-dependent 14-demethylase result in decreased affinity for azole antifungals. Biochem. Soc. Trans. **18**, 124–126 (1990)
4. Nosanchuk, D.J.: Current status and future of antifungal therapy for systemic mycoses. Recent Patents Anti-Infect. Drug Disc. **1**, 36–41 (2006)
5. Hitchcock, C.A., Barret Bee, K.J., Rusell, N.J.: The lipid composition and permeability to azole of an azole and polieneresistant mutant of *Candida albicans*. J. Med. Vet. Micol. **25**, 29–37 (1987)
6. Stoescu, V.: Bazele farmacologice ale practicii medicale. *Editura Medicala- Bucuresti*, ed. a 7-a, rev. si compl (2001)
7. Higuchi, T., Connors, K.A.: Phase-solubility techniques. Adv. Anal. Chem. Instr. **4**, 212–217 (1965)
8. Manca, M.L., Zaru, M., Ennas, G., Valenti, D., Sinico, C., Loy, G., Fadda, A.M.: Diclofenac-β-cyclodextrin binary systems: physicochemical characterization and in vitro dissolution and diffusion studies. AAPS PharmSciTech. **6**(3), 464–472 (2005)
9. Mukne, A.P., Nagarsenker, M.S.: Triamterene-β-cyclodextrin systems: preparation, characterization and in vivo evaluation. AAPS PharmSciTech. **5**(1), 1–9 (2004)
10. Piel, G., Dive, G., Ervard, B., Van Hees, T., Henry de Hassonville, S., Delattre, L.: Molecular modeling study of β- and γ-cyclodextrin complexes with miconazole. Eur. J. Pharm. Sci. **13**, 271–279 (2001)
11. Redenti, E., Fronza, G., Spisni, A.: Nuclear overhauser effect, a powerful tool for the investigation of the geometry in solution of different inclusion complexes with β-cyclodextrin. Minutes Int. Symp. Cyclodextrins 220–225 (1992)
12. Mulinacci, N., Melani, F., Vincieri, F.F., Mazzi, G., Romani, A.: 1H-NMR NOE and molecular modelling to characterize thymol and carvacol (-cyclodextrin complexes. Int. J. Pharm. **128**, 81–88 (1995)
13. Morin, N. et al.: Formation of two particular structures between (-cyclodextrin and bifazole: (-CD-bifonazole (where $2 < i < 3$). J. Chem. Soc. Perkin. Trans. **2**, 2647–2651 (1999)